

Supplementary Materials

High-resolution solid-state NMR spectroscopy of hydrated non-crystallized RNA.

Sha Zhao^{†a,b}, Yufei Yang^{†a,b}, Yujie Zhao^{a,b}, Xinming Li^c, Yi Xue^c, and Shenlin Wang^{*a,b,d}

a. College of Chemistry and Molecular Engineering, Peking University, Beijing, 100871, China

b. Beijing NMR Center, Peking University, Beijing, 100871, China

c. School of Life Sciences; Tsinghua-Peking Joint Center for Life Sciences; Beijing Advanced Innovation Center for Structural Biology; Beijing Frontier Research Center for Biological Structure, Tsinghua University, Beijing, 100084, China.

d. Beijing National Laboratory for Molecular Sciences, Beijing, China

[†] These authors contributed equally.

* Correspondence and requests for materials should be addressed to S.W. (e-mail: wangshenlin@pku.edu.cn)

1. Experimental Procedures

1.1 Materials

The ¹⁵N,¹³C-labeled rNTP reagents were purchased from Cambridge Isotope Laboratories (Andover, MA). The DNA templates for the *in vitro* transcription reactions were purchased from BGI company (Beijing, China), GENEWIZ company (Tianjin, China) or Sangon Biotech company (Shanghai, China).

1.2 In Vitro Transcription Reaction and Purification of RNA

Two RNAs were prepared to evaluate the applicability of the ethanol-precipitation approach to obtaining precipitated RNA that yields high-quality SSNMR spectra. These RNAs include a genomic RNA from the dimerization initiation site of HIV-1 (DIS-HIV-1) and an adenine riboswitch (riboA71). DIS-HIV-1 is a 26 nt HIV genome RNA, which is critical in HIV-1 virus life cycles and is a potential antiviral drug target.¹ RiboA71 is the 71-nt aptamer domain of the *add* adenine riboswitch, which regulates the expression of the *add* gene.²

The uniform ¹⁵N,¹³C-labeled DIS-HIV-1 with the sequence of 5'-GGGCUUGCUGAGGUGCACACAGCAAG-3' was prepared using the previously reported protocol.³ The DNA template with sequence 5'-TTAATACGACTCACTATAGGGCTTGCTGAGGTGCACACAGCAAG-3' and its complementary sequence were dissolved and annealed by heating at 95 °C to obtain a duplex template. The reaction materials, containing 5 mM ¹⁵N,¹³C-labeled rNTPs, 40 mM Tris-HCl (pH 7.0), 0.01% Triton X-100, 1 mM spermidine, 10 mM DTT, 50 mM MgCl₂, 0.3 μM DNA template and 0.1 mg/mL T7 RNA polymerase, were incubated at 37 °C for 24 h. The final RNA product was purified using 16% polyacrylamide gel electrophoresis (PAGE). The yield of the purified DIS-HIV-1 was ~5 mg per 10 mL of reaction system. Early studies showed that DIS-HIV-1 forms dimers in solutions containing cations and exists as a monomer in water. In this work, the purified DIS-HIV-1 was buffer-exchanged into a pH 7.0 buffer containing 20 mM sodium cacodylate, 5 mM MgCl₂, 150 mM KCl, and 5 mM spermidine and then annealed to form dimers. To prepare monomeric DIS-HIV-1, the RNA was buffer-exchanged into water and then annealed as described previously.

The uniform ¹⁵N,¹³C-labeled riboA71 with the sequence of 5'-GGGAAGAUAAUCCUAAUGAU AUGGUUUGGAGUUUCUACCAAGAGCCUAAACUCUUGAUUUAU CUUCCC-3' was prepared using *in vitro* transcription. The DNA templates were prepared by annealing single-stranded DNA with the sequence 5'-TTAATACGACTCACTATAGGGAAGATATAATCCTAATGATATGGTTTGGGAGTTTCTACCAAGAGCCT TAAACTCTTGATTATCTTCCC-3' and its complementary sequence at 95 °C for 10 min. The *in vitro* transcription reaction materials containing 5 mM ¹⁵N,¹³C-labeled rNTPs, 40 mM Tris-HCl (pH 7.0), 0.01% Triton X-100, 1 mM spermidine, 10 mM DTT, 45 mM MgCl₂, 0.85 μM DNA template and 0.12 mg/mL T7 RNA polymerase were incubated at 37 °C for 24 h. The synthesized RNA was purified using 12% PAGE under denaturing conditions and eluted from the gel with buffer containing 20 mM Tris-HCl, 300 mM sodium acetate, 1 mM EDTA, pH 7.4. The final yield of the purified RNA sample was ~5 mg per 10 mL of reaction system. Purified riboA71 was buffer-exchanged into a pH 6.8 buffer containing 10 mM KH₂PO₄, 30 mM KCl, 2 mM MgCl₂, and concentrated to a final concentration of 700 μM. To

prepare the complex of the riboA71 and the adenine, the adenine stock was added to the riboA71 solution to a final concentration of 5 mM, followed by annealing at 95 °C for 5 min and then incubation at 0 °C for 30 min.

1.3 Preparation of Partially Deuterated RNA Samples

Partial deuteration can improve the spectral resolution of ^1H -detected solid-state NMR spectra. To produce the partially deuterated RNA samples, the ^{15}N , ^{13}C -labeled RNAs were annealed in 75% D_2O /25% H_2O (v/v)-based buffer to achieve the H/D exchange of the imino and the imide protons to a desired level, followed by buffer exchange into the targeted conditions. To obtain ethanol-precipitated partially deuterated samples for SSNMR, the partially deuterated RNAs were precipitated by adding the pre-chilled ethanol stock consisting of 75% $\text{C}_2\text{D}_5\text{OD}$ /25% $\text{C}_2\text{H}_5\text{OH}$ (v/v), and using the procedure discussed in section 1.4. The final concentrations of ethanol in solution were 75%. Other reagents and experimental procedures were conducted identically to those used to prepare ethanol-precipitated H_2O -based RNA precipitates.

1.4 Preparation of ethanol-precipitated RNA Samples for SSNMR Studies

The scheme for the preparation of ethanol-precipitated RNA is illustrated in Figure 1, and was used for precipitation of all RNAs in this study. About 4 mg of ^{15}N , ^{13}C -labeled RNA was concentrated to approximately 13 mg/mL in a final volume of approximately 300 μL . 30 μL of 2 M NaCl solution was added to the RNA solution. Subsequently, 900 μL pre-chilled ethanol was added to the solution and the mixture was incubated at -20 °C overnight to yield RNA precipitation. The RNA pellets were collected by centrifugation at 9600 g for 3 min. The pellet was central-packed by centrifugation into a 1.9 mm rotor for SSNMR studies.

To evaluate the yield of RNA precipitation by ethanol, 100-200 μg of RNA was precipitated and then re-dissolved in water. The quantitative analysis of re-dissolved RNA was monitored by UV absorbance spectroscopy at 260 nm. Two replicate experiments were performed for each sample, and showed an average of ~90% recovery.

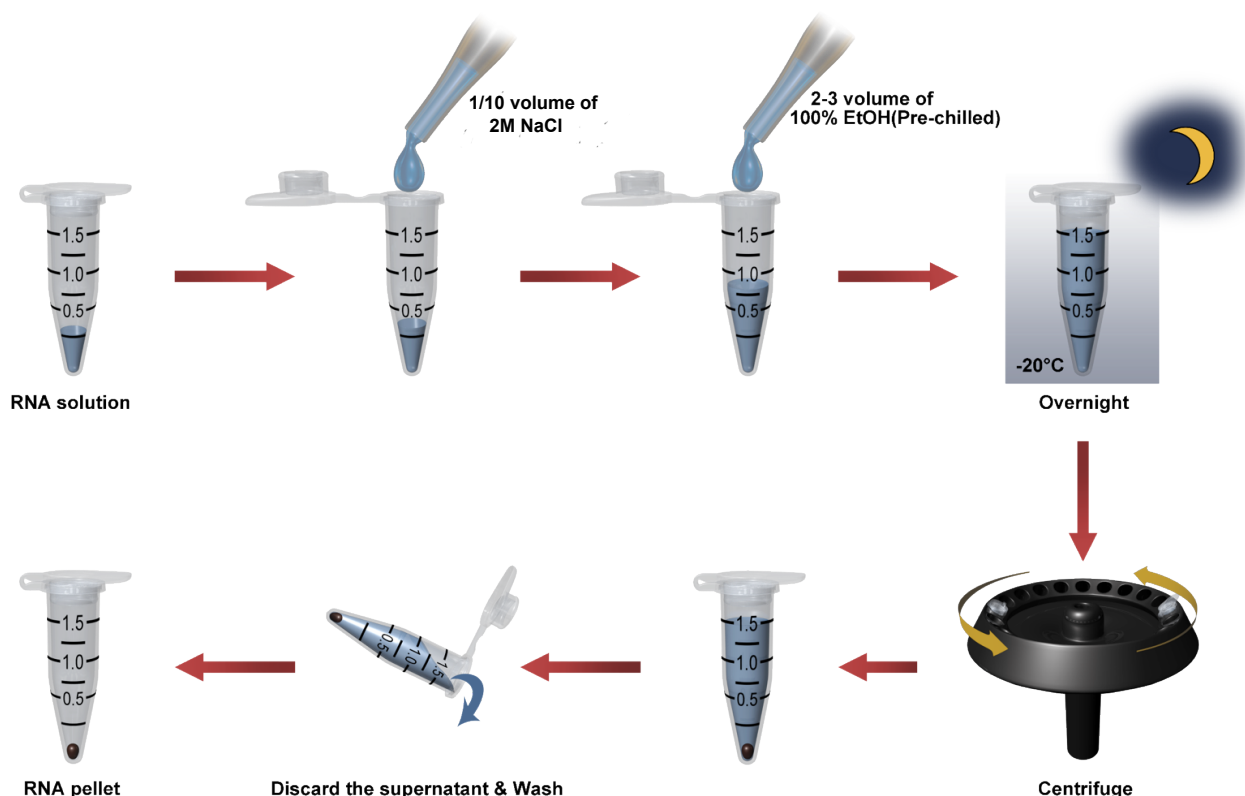


Figure 1. Workflow of the strategy for ethanol-precipitated RNA sample preparation.

1.5 Preparation of crystallized DIS-HIV-1

Microcrystalline DIS-HIV-1 was produced according to a previously reported protocol.³ The dimeric RNA samples were incubated at 37 °C for 2 h, followed by the addition of a precipitant solution (50 mM spermine and 10% methyl pentanediol (MPD)) at a ratio of 10% (v/v) and an equal volume of reservoir solution (50% MPD, 50 mM sodium

cacodylate, 100 mM MgCl₂, and 300 mM KCl). The RNA precipitate appeared rapidly and was collected after an overnight incubation at 4 °C.

1.6 Solid-state NMR Spectroscopy

Approximately 4 mg of the ethanol-precipitated DIS-HIV-1 RNA or riboA71 was center-packed into a 1.9 mm rotor by centrifugation. All the SSNMR experiments were performed on a 600 MHz Bruker Avance III spectrometer, equipped with a 1.9 mm triple-resonance ¹H-X-Y MAS probe. Unless otherwise indicated, all experiments were conducted with a MAS rate of 40 kHz and at an effective temperature of 5 °C. The temperature was calibrated using the *T*₁ relaxation rate of ⁷⁹Br in KBr powder.⁴

The typical $\pi/2$ pulse lengths were 2.0 μ s for ¹H, 4.0 μ s for ¹³C, and 5.0 μ s for ¹⁵N. Low-power TPPM proton decoupling (nutating frequency \sim 10 kHz) was used during the ¹⁵N or the ¹³C chemical shift evolution,⁵ and WALTZ-16 decoupling (nutating frequency \sim 10 kHz) on the ¹⁵N and the ¹³C was used during the evolution of the proton chemical shift. The MISSISSIPPI pulse trains were applied to suppress the solvent signal of the dipolar-based ¹H-detected experiments.⁶ The recycle delays of all SSNMR experiments were set to 2.0 s.

The 1D ¹H-X (X = ¹³C, ¹⁵N or ³¹P) CP experiments were recorded with a constant lock field of the X channel at 50 kHz and with the proton field ramped linearly around $n = 1$ Hartmann-Hahn conditions.⁷ The contact times were 2.0 ms for ¹H-³¹P CP, 2.5 ms for ¹H-¹³C CP, and 4.0 ms for ¹H-¹⁵N CP, respectively. The 1D ¹H-¹³C, ¹H-¹⁵N and ¹H-³¹P CP spectra were recorded with 32, 2048, and 32 scans, respectively.

The dipolar-based 2D hNH experiments (Figure. 2a) were recorded using the pulse sequence published previously.⁶ The initial ¹H-¹⁵N and ¹⁵N-¹H CP was set with a constant lock field of 50 kHz on ¹⁵N and with the proton field ramped linearly around 90 kHz. The contact times of the ¹H-¹⁵N and ¹⁵N-¹H CP were set at 4 ms and 400 ms, respectively. The carrier frequencies were set at 10 ppm for ¹H and 155 ppm for ¹⁵N, respectively. The hNH experiments were recorded with 32 scans for the H₂O-based RNA and 48 scans for the partially deuterated RNA, respectively. The time domain matrixes of the 2D hNH experiments were 300 (*t*₁) \times 1024 (*t*₂), leading to total acquisition times of 15 ms for ¹⁵N and 20 ms for ¹H, respectively.

The 2D ¹⁵N-¹³C experiments, hNC (Figure. 2b), were recorded using the pulse sequence published previously.⁸ The initial ¹H-¹⁵N was set identically as used in the ¹H-¹⁵N CP experiments. The ¹⁵N-¹³C SPECIFIC CP⁸ were set with contact times of 6 ms, and constant lock field of 50 kHz on ¹⁵N and ¹³C field ramped linearly around 90 kHz. The carrier frequencies were placed at 10 ppm for ¹⁵N and 155 ppm for ¹³C, respectively. The 2D hNC experiments were recorded with 32 scans. The time domain matrixes of the 2D hNC experiments were 300 (*t*₁) \times 1024 (*t*₂), leading to total acquisition times of 15 ms for ¹⁵N and 20 ms for ¹³C, respectively.

The ¹H-detected 2D ¹H-¹⁵N correlation experiments, hCNH and hCN(PAR)NH (Figure. 2c, d), were recorded with the ethanol-precipitated DIS-HIV-1 to evaluate the Watson-Crick base-pairing in ethanol-precipitated RNA, using the pulse sequences published previously.³ The initial ¹H-¹³C CP contact time was 2.0 ms, with constant lock field of 60 kHz on ¹³C and the proton field ramped linearly around 100 kHz. The ¹³C-¹⁵N SPECIFIC CP transfers were implemented with a contact time of 5.5 ms,⁸ with a constant lock field of 15 kHz on ¹³C and a ¹⁵N lock field ramped linearly (10%) around 25 kHz. The carrier frequencies were placed at 160 ppm for ¹³C and 190 ppm for ¹⁵N, respectively. The ¹⁵N-¹⁵N PAR⁹⁻¹¹ transfer was set with contact time of 7 ms, and with a constant lock field of 26 kHz and 67 kHz on the ¹⁵N and ¹H channels, respectively. The hCNH and the hCN(PAR)NH were recorded with 64 and 100 scans, respectively.

All the NMR data were processed using the TOPSPIN program. The spectra were analyzed using CARR. Chemical shifts were referenced to 2,2-dimethyl-2-silapentane-5-sulfonic acid (DSS), using adamantane as a secondary standard.¹² The ¹H and ¹⁵N chemical shifts were referenced indirectly using $\gamma^3\text{C}/\gamma\text{H} = 0.25145020$ and $\gamma^5\text{N}/\gamma^{13}\text{C} = 0.40297994$, respectively.

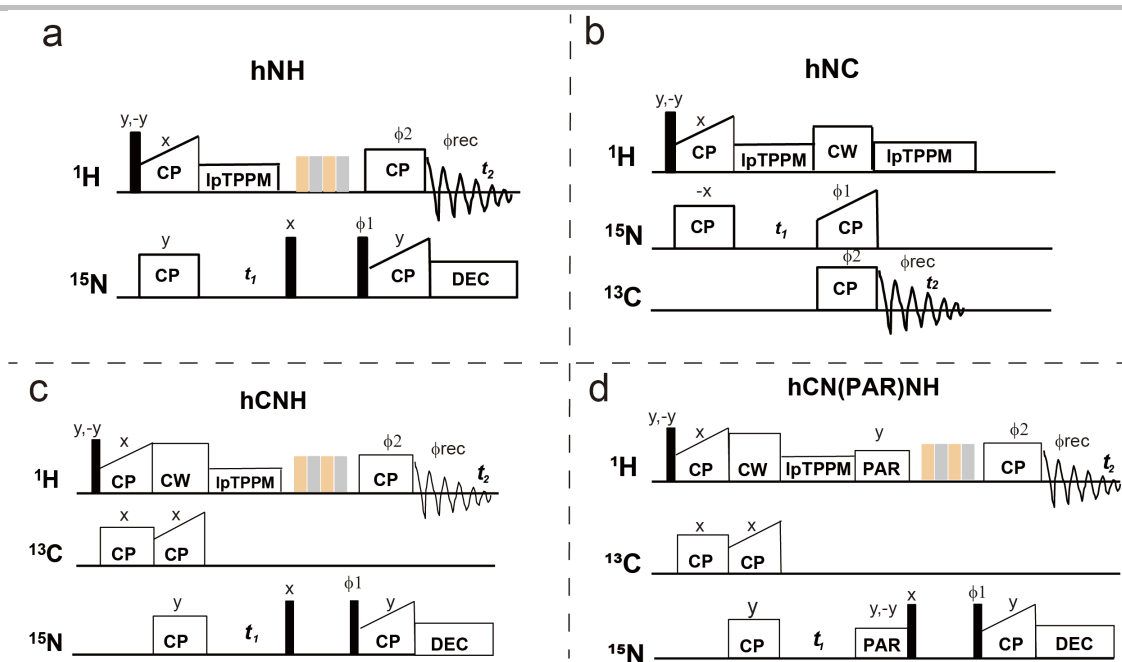


Figure 2. Pulse sequences for 2D SSNMR experiments, including (a) 2D hNH experiment, (b) 2D hNC experiment, (c) 2D hCNH experiment and (d) 2D hCN(PAR)NH experiment. For all the pulse sequences, filled black bars and open bars represent $\pi/2$ and π pulses, respectively. The yellow and gray bars represent the water suppression period using MISSISSIPPI pulse trains⁶. The pulse phases are indicated on the pulse, with the exception of the following: (a, c, d) $\phi_1 = (x, x, -x, -x)$, $\phi_2 = (y, y, y, y, -y, -y, -y, -y)$, and $\phi_{rec} = (y, -y, -y, y, -y, y, y, -y)$; (b) $\phi_1 = (x, x, -x, -x)$, $\phi_2 = (x, x, y, y, -x, -x, -y, -y)$, and $\phi_{rec} = (-x, x, y, -y, x, -x, -y, y)$. The TPPI phase-sensitive detection was obtained in the indirect t_1 dimension by incrementing the first $\pi/2$ pulse phase of the ^{15}N channel (a,c,d) or incrementing the first spin-lock pulse phase of the ^{15}N channel (b).

2. Results and Discussion

2.1 Comparison of ^{31}P SSNMR Spectra of the Crystallized and the Ethanol-precipitated DIS-HIV-1

The 1D ^{31}P spectra of the DIS-HIV-1 were collected for different sample forms, i.e., the crystallized form, the precipitated form and the lyophilized form. Figure 3a compares the 1D ^{31}P spectra of the dimeric DIS-HIV-1 in crystals and in ethanol-precipitated pellets, showing that the two samples yield ^{31}P spectra with similar resolutions. The linewidth of the ^{31}P spectra of both the crystallized and the precipitated sample is about 1.5 ppm, corresponding to ~ 360 Hz. In comparison, the ^{31}P spectrum of the lyophilized DIS-HIV-1 was also recorded and showed a linewidth of 2.4 ppm, corresponding to ~ 590 Hz, which is 1.6-fold broader than that of the crystallized RNA (Figure 3b). This shows that the spectral resolution of the precipitated RNA sample is comparable to that of the crystallized sample, while the lyophilized RNA samples exhibit much broader linewidth.

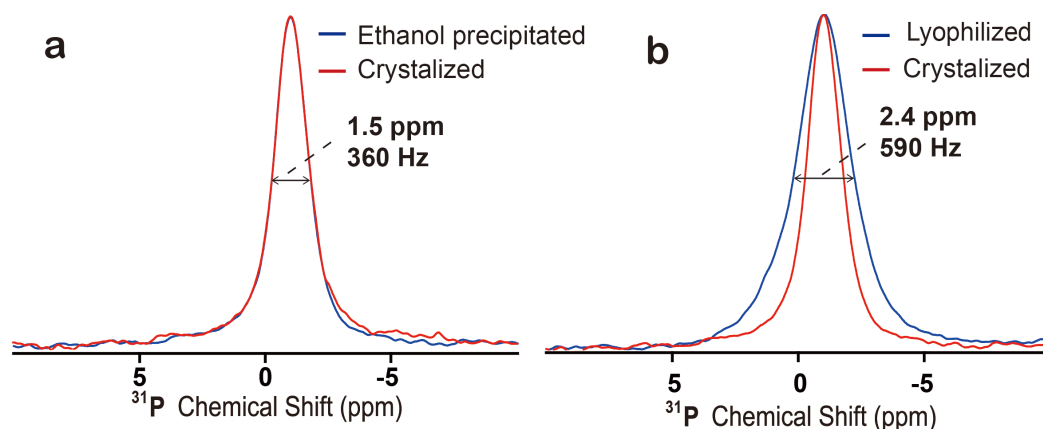


Figure 3. Comparison of spectral resolution of DIS-HIV-1 in different sample forms. (a) Overlay of ^{31}P spectra of the crystallized DIS-HIV-1 (blue) and the precipitated DIS-HIV-1 (red). (b) Overlay of ^{31}P spectra of the crystallized DIS-HIV-1 (red) and the lyophilized DIS-HIV-1 (blue).

2.2 Spectral Resolution of SSNMR Spectra of Ethanol-precipitated RNAs

The 1D ^{15}N and 1D ^{13}C spectra of the ethanol-precipitated RNA samples were recorded to evaluate the resolution of the ^{15}N and ^{13}C spectra. A comparison of the 1D ^{15}N and ^{13}C spectra between the crystallized DIS-HIV-1 and the ethanol-precipitated DIS-HIV-1 identified similar patterns and spectral quality. Nevertheless, some cross peaks exhibited different peak heights, which may be caused by different packing conditions of crystallization and ethanol precipitation (Figure. 4). The overall spectral quality of riboA71 is also similar to that of DIS-HIV-1, again confirming the applicability of ethanol-precipitation approach to achieve high-resolution SSNMR spectra of RNA.

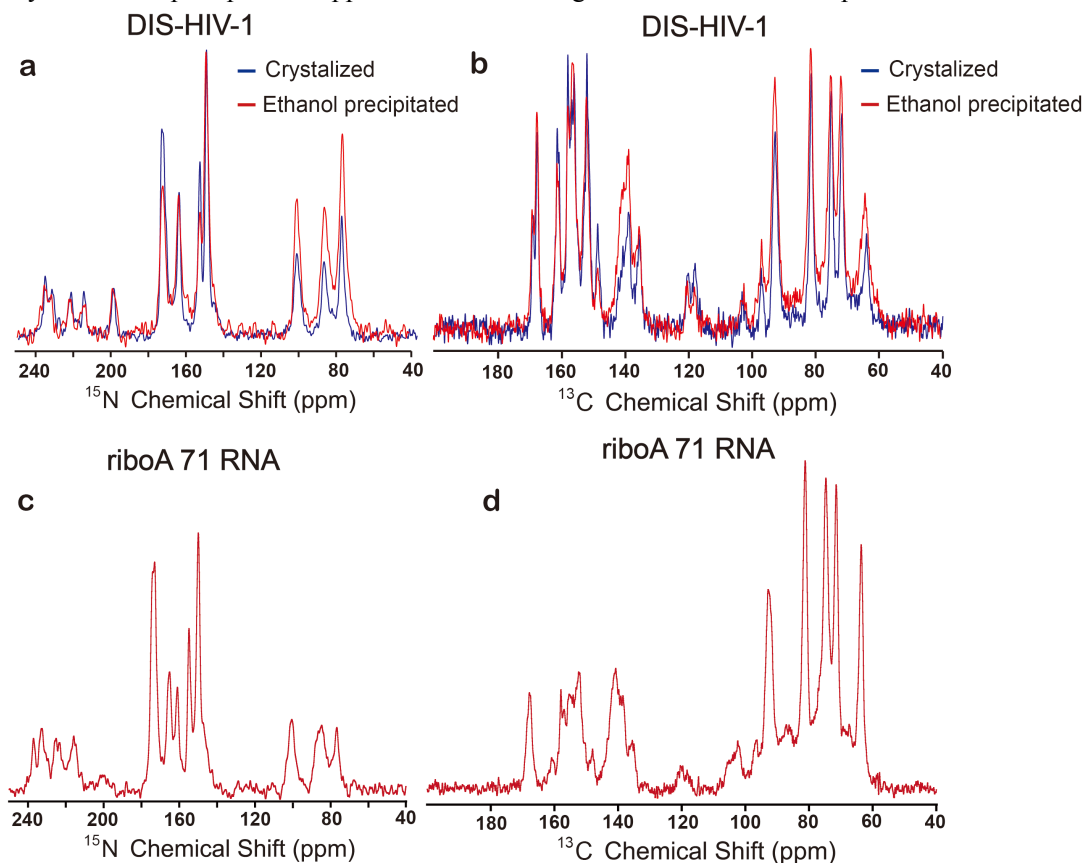


Figure 4. The 1D ^{13}C and 1D ^{15}N SSNMR spectra of DIS-HIV-1 and riboA71. (a) Overlay of ^{15}N spectra of the crystallized (blue) and ethanol-precipitated DIS-HIV-1 (red). (b) Overlay of ^{13}C spectra of the crystallized (blue) and the ethanol-precipitated DIS-HIV-1 (red). (c-d) 1D ^{15}N (c) and ^{13}C (d) spectrum of the ethanol-precipitated riboA71.

To further evaluate the SSNMR spectra quality of ethanol-precipitated RNA, we collected 2D hNC spectra for the two RNA samples (Figure 2 in the manuscript). Besides, the 2D ^{15}N - ^{13}C spectra of the crystallized DIS-HIV-1 was also collected (Figure 5), which identified similar patterns and spectral quality with respect to the ethanol-precipitated DIS-HIV-1. The nucleotide-type specific assignments are highlighted in different colors, with one-bond ^{15}N - ^{13}C correlations highlighted in blue and long-range ^{15}N - ^{13}C correlations highlighted in red. The ^{13}C and ^{15}N chemical shifts for each of the peaks are listed in Table 1.

The 2D ^{15}N - ^{13}C spectra of the two RNA samples were collected to detect the intra-nucleotide correlations. The nucleotide-specific assignments were obtained using the statistics from BMRB (http://www.bmrb.wisc.edu/ref_info/). The ^{15}N chemical shifts were assigned for the amino group of G-N2 at 75 ppm, the C-N4 at 98 ppm, and the A-N6 at 94 ppm. These ^{15}N resonances were well-resolved, allowing unambiguous assignments of the intra-nucleotide one-bond ^{15}N - ^{13}C correlations of the G-C2/N2, the A-C6/N6, and the C-C4/N4 (Figure. 2 in the manuscript and Table 1). The C-N1 has a chemical shift of 152 ppm, with detection of three cross peaks. One of the cross peaks can be assigned to C-C4/N1 by linking C-C4/N4 peaks, and the other two cross peaks are C-C2/N1 and C-C6/N1, obtained with characteristic ^{13}C chemical shifts of C2 of 159 ppm and C6 of 142 ppm. The U-N3 of uridine has a chemical shift of 162 ppm, allowing the assignments of U-C4/N3 and U-C2/N3. The chemical shifts of the U-N1 and the G-N1 are close to each other. The U-C4/N1 can be assigned by correlating the U-C4/N3 with the U-C4/N1, while the other cross peaks involving G-N1 or U-N1 were obtained by correlating the characteristic ^{13}C chemical shifts of the nucleotide.

No.	^{13}C ppm	^{15}N ppm	Assignments
1	156.6	75.2	Guanosine N2/C2
2	161.8	75.2	Guanosine N2/C6
3	158.1	84.3	Adenosine N6/C6
4	168.8	97.6	Cytidine N4/C4
5	159.0	97.6	Cytidine N4/C2
6	168.6	147.5	UridineN1/C4
7	161.8	147.6	Guanosine N1/C6
8	156.6	147.6	Guanosine N1/C2
9	152.9	147.6	Guanosine N1/C4or UridineN1/C2
10	142.0	147.5	UridineN1/C6
11	168.8	151.9	Cytidine N1/C4
12	159.0	151.9	Cytidine N1/C2
13	142.0	151.9	Cytidine N1/C6
14	168.6	163.0	UridineN3/C4
15	152.9	163.0	UridineN3/C2

Table 1. The ^{13}C and ^{15}N nucleotide specific assignments

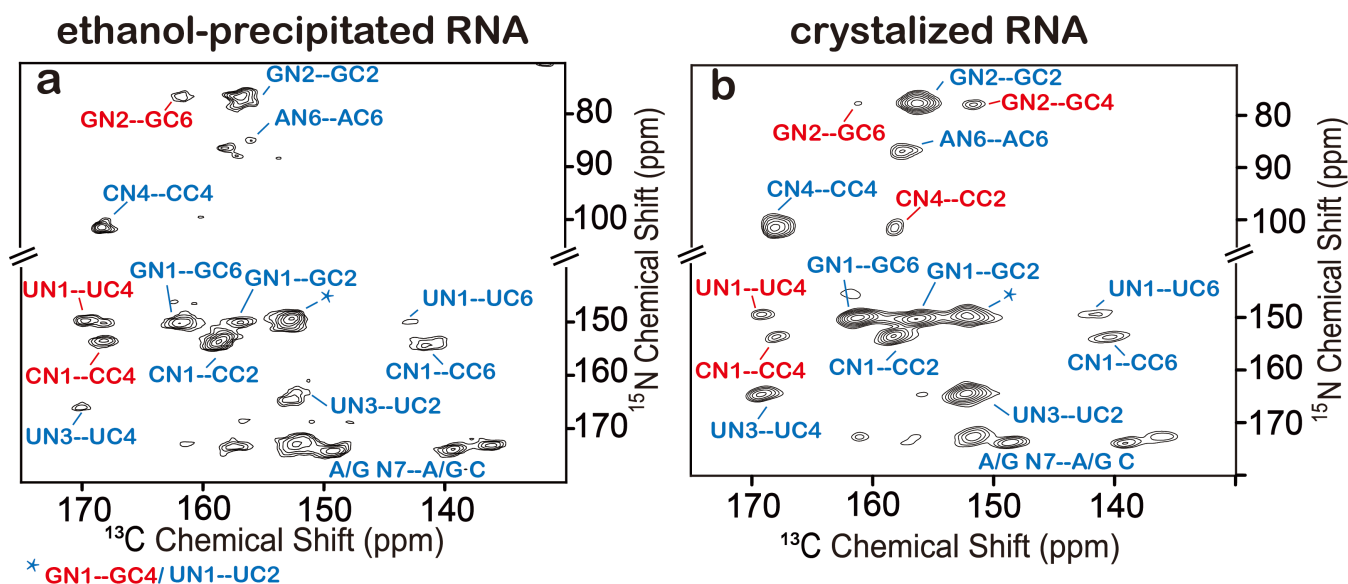


Figure 5. 2D ^{15}N - ^{13}C spectra of ethanol-precipitated DIS-HIV-1(a) and crystallized DIS-HIV-1(b).

2.3 Partial H/D Exchange Improves the Resolution of the ^1H -detected SSNMR.

The ^1H -detected 2D hNH spectra were recorded to evaluate the proton linewidth of ethanol-precipitated RNA and the effects of ethanol on the structure of the RNAs. Strong proton-proton dipolar couplings make the major homogeneous broadening contributions to proton linewidth in SSNMR spectra. Partial deuteration on RNA improves the proton resolution of SSNMR. Here, partially deuterated RNA samples were prepared by H/D exchange, through annealing RNA in 75% D_2O /25% H_2O (v/v)-based buffer, followed by the ethanol-precipitation step. In this method, some of the imino and the amide protons are replaced by deuterons, thus removing the strong inter-proton dipolar couplings between the exchangeable protons involving the H-bonds of base pairs. As tested, the hNH spectra of partial ^2D DIS-HIV-1 showed a proton linewidth of 230 Hz for the proton of the GN1-GH1 with $^1\text{H}/^{15}\text{N}$ chemical shift of 12 ppm and 147.5 ppm, which is 300 Hz smaller than that from a fully protonated sample (Figure 6). As observed in the riboA71 spectra, the well-resolved cross peak represents the linewidth of 130 Hz. Those values are consistent with the linewidth of the partially deuterated proteins as measured at the same MAS rate¹³, showing the high-quality spectra from ethanol-precipitated RNA.

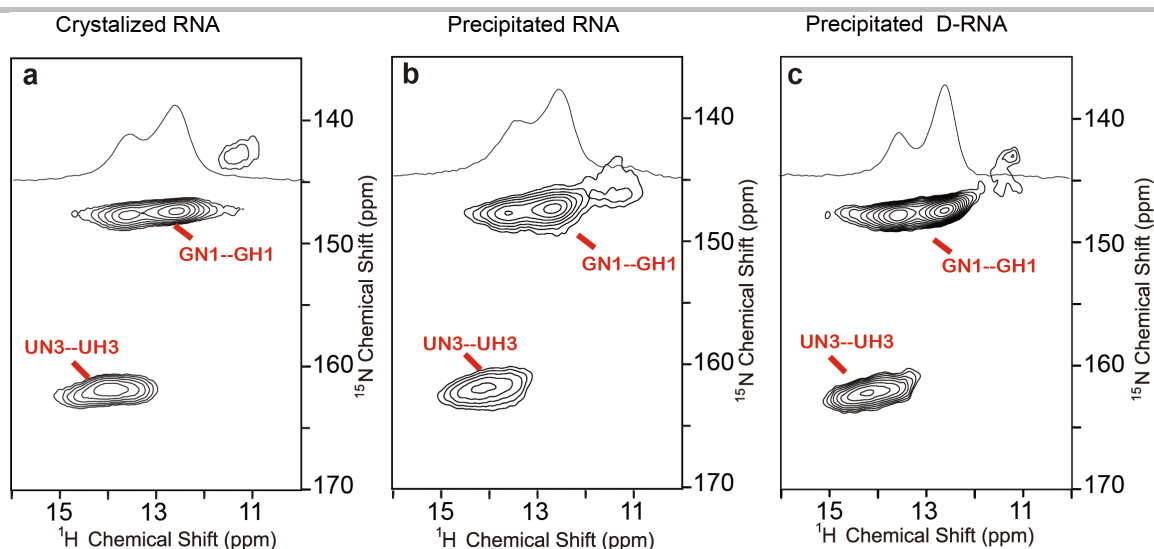


Figure 6. Comparison of the 2D ^1H - ^{15}N spectra of DIS-HIV-1 in different forms. (a) 2D ^1H - ^{15}N spectra of the crystallized DIS-HIV-1. (b) 2D ^1H - ^{15}N spectra of the ethanol-precipitated DIS-HIV-1. (c) 2D ^1H - ^{15}N spectra of the ethanol-precipitated DIS-HIV-1 with partial deuteration. The nucleotide-type specific assignments are highlighted in red.

The 2D hNH spectra of both the DIS-HIV-1 and the riboA71 exhibit the cross peaks of the imino groups involving canonical A-U and G-C base pairs. The cross peaks with $^1\text{H}/^{15}\text{N}$ chemical shift at 12 ppm/147.5 ppm were assigned to N1-H1 groups of guanosines within the G-C canonical base pairs. The N3/H3 imino groups of the uridines in the A-U canonical base pairs were identified by their $^1\text{H}/^{15}\text{N}$ chemical shifts of 14 ppm/162 ppm. To confirm the presence of the canonical base pairs in ethanol-precipitated RNA, the 2D hCNH and 2D hCN(PAR)NH experiments were also collected on fully protonated DIS-HIV-1. As shown in Figure 6-7, the characteristic resonances for both the GC and the AU base pairings were detected, confirming the presence of the canonical base pairing of DIS-HIV-1 in ethanol precipitated form. It is noted that the bulk peak intensity of the GC pairs is stronger than that of the AU pairs. This is because the number of the GC pairs is more than that of the AU pairs. According to the structure of the DIS-HIV-1, the DIS-HIV-1 has four GC pairs and three AU pairs. Nevertheless, the yield of the PAR polarization transfer of both the GC and the AU pairs are $\sim 30\%$.

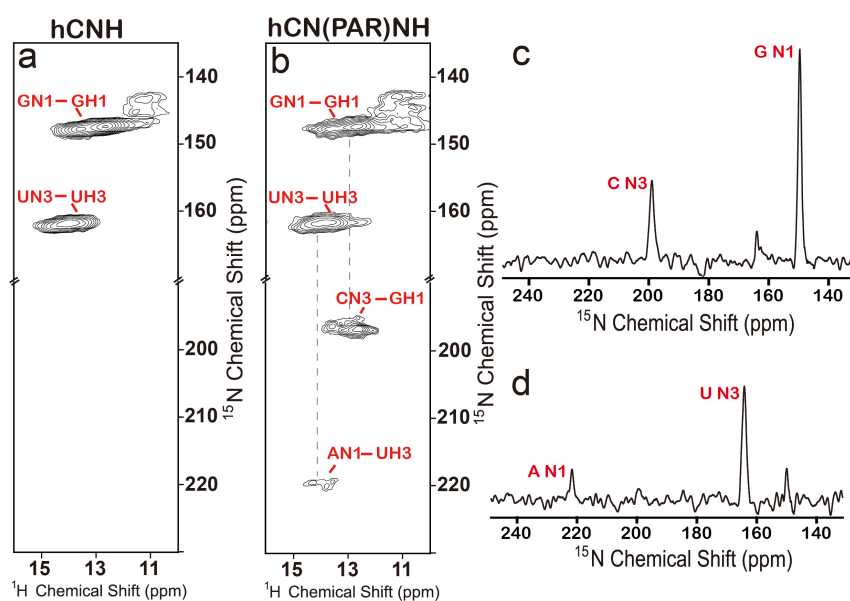


Figure 7. 2D ^1H -detected ^1H - ^{15}N spectra of the DIS-HIV-1. (a-b) The 2D hCNH (a) and 2D hCN((PAR)NH (b) of the monomeric DIS-HIV-1. The nucleotide-type specific assignments are highlighted in red. The cross-peaks illustrating the GC and the AU base pairs are connected by dashed gray lines. (c-d) The 1D slices corresponding to the GC pairs and the AU pairs are extracted at 1H chemical shift of 12.8 ppm (c) and 14.0 ppm (d), respectively.

For riboA71, both the canonical and the non-canonical base pairs were observed in the 2D hNH spectra. Notably, a comparison of the HSQC spectra of riboA71 in solution and the dipolar-based 2D hNH of solid riboA71 showed similar overall patterns for the GC and the AU base pairs (Figure 8). The well-resolved peaks were assigned according to the assignments of riboA71 in solution. The imino group of G30 in the non-canonical G-U base pair was observed with a $^1\text{H}/^{15}\text{N}$ chemical shift of 10.0 ppm/142.7 ppm, and forms G-U base pairs with U16. Both cross-peaks are well-resolved in solid-state NMR spectrum.

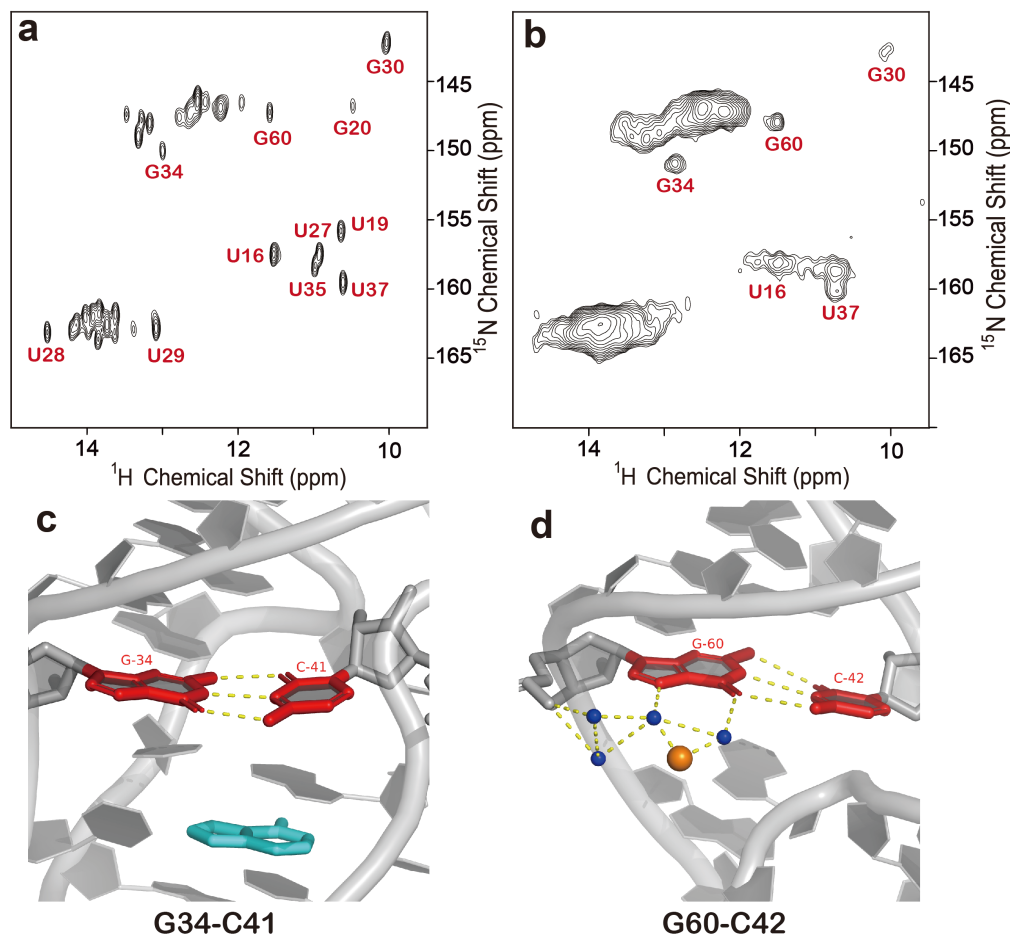


Figure 8. A comparison of the solution and the solid-state NMR spectra of the riboA71. (a) The ^1H - ^{15}N HSQC spectrum of the riboA71 in solution, with part of the assignments highlighted. (b) The dipolar based 2D hNH SSNMR spectrum of riboA71, with the well-resolved cross-peaks highlighted. (c-d) The base pairs of G34-C41 (c) and G60-C42 (d) are mapped on the structure of riboA71 (PDB code: 4TZX).

3. References

1. E. Ennifar, P. Walter, B. Ehresmann, C. Ehresmann and P. Dumas, *Nat Struct Biol*, 2001, **8**, 1064-1068.
2. J. R. Stagno, Y. Liu, Y. R. Bhandari, C. E. Conrad, S. Panja, M. Swain, L. Fan, G. Nelson, C. Li, D. R. Wendel, T. A. White, J. D. Coe, M. O. Wiedorn, J. Knoska, D. Oberthuer, R. A. Tuckey, P. Yu, M. Dyba, S. G. Tarasov, U. Weierstall, T. D. Grant, C. D. Schwieters, J. Zhang, A. R. Ferre-D'Amare, P. Fromme, D. E. Draper, M. Liang, M. S. Hunter, S. Boutet, K. Tan, X. Zuo, X. Ji, A. Barty, N. A. Zatsepin, H. N. Chapman, J. C. Spence, S. A. Woodson and Y. X. Wang, *Nature*, 2017, **541**, 242-246.
3. Y. Yang, S. Xiang, X. Liu, X. Pei, P. Wu, Q. Gong, N. Li, M. Baldus and S. Wang, *Chem Commun (Camb)*, 2017, **53**, 12886-12889.
4. K. R. Thurber and R. Tycko, *J Magn Reson*, 2009, **196**, 84-87.
5. K. Sharma, P. K. Madhu and V. Agarwal, *J Magn Reson*, 2016, **270**, 136-141.
6. D. H. Zhou and C. M. Rienstra, *J Magn Reson*, 2008, **192**, 167-172.
7. S. R. Hartmann and E. L. Hahn, *Phys Rev*, 1962, **128**, 2042-&.
8. S. Jehle, K. Rehbein, A. Diehl and B. J. van Rossum, *J Magn Reson*, 2006, **183**, 324-328.
9. G. De Paepe, J. R. Lewandowski, A. Loquet, A. Bockmann and R. G. Griffin, *J Chem Phys*, 2008, **129**, 245101.
10. J. R. Lewandowski, G. De Paepe, M. T. Eddy, J. Struppe, W. Maas and R. G. Griffin, *J Phys Chem B*, 2009, **113**, 9062-9069.
11. J. R. Lewandowski, G. De Paepe, M. T. Eddy and R. G. Griffin, *J Am Chem Soc*, 2009, **131**, 5769-5776.
12. C. R. Morcombe and K. W. Zilm, *J Magn Reson*, 2003, **162**, 479-486.
13. V. Chevelkov, A. Diehl and B. Reif, *Magn Reson Chem*, 2007, **45 Suppl 1**, S156-160.